

A Comparative Molecular Orbital Study and Vibrational Analysis of Bis(Diethyldithiophosphato) Nickel(II) and its Pyridine Adduct

P. K. GOGOI* and R. KONWAR

Department of Chemistry, Dibrugarh University, Dibrugarh-786 004, India

Unlike the coordinatively unsaturated NiS_4 core of bis(diethyldithiocaramato) nickel(II), bis(diethyldithiophosphato) nickel(II) readily forms bis-pyridine (Py) adduct with distortion of chelate rings but maintaining their coplanarity. The adduct formation is facilitated by donation of electrons from the highest occupied molecular orbital, HOMO [$N(p_z)$] of pyridine to the lowest unoccupied molecular orbital, LUMO [$Ni(d_z^2)$] of nickel(II) diethyldithiophosphate. As a result of adduct formation and concomitant coordination expansion, the Ni-S bond length and S—P—S bond angle are increased while the S—Ni—S bond angle is decreased. These changes are attributed to the decrease of net positive charge on the nickel atom with a simultaneous increase of net negative charges on the sulfur atoms.

The former effect increases the Ni—S bond length resulting in a decrease of S—Ni—S bond angle while the latter effect increases the S—P—S bond angle. These structural changes cause a considerable change in the properties of the resulting adduct. A comparative Extended Huckel Molecular Orbital (EHMO) study of $[Ni\{S_2P(OC_2H_5)_2\}_2]$ and its pyridine adduct is, therefore, made to elucidate the effect of adduct formation on the bonding characteristics of the parent complex by calculating the net charges (Q) on individual atoms, reduced overlap populations (ROP) between different atom pairs as well as by fragment molecular orbital (FMO) analysis. The EHMO results, thus obtained, have been correlated to the relevant force constants (f) and IR frequencies determined by normal coordinate analysis (NCA). There is good agreement between the calculated and the observed frequencies which are assigned by the potential energy distribution (PED) calculation.

Key Words: EHMO, NCA, Bis-pyridine adduct, Bis(diethyl dithiophosphato)nickel(II).

INTRODUCTION

Diamagnetic, square-planar dithiophosphato, dithiophosphinato and xanthato complexes of nickel(II) with coordinatively unsaturated NiS_4 cores easily expand their coordination spheres by forming paramagnetic, octahedral adducts with suitable N-donors, while dithiocarbamate analogues rarely form such adducts¹. In an earlier communication from this laboratory the reasons for such different

behaviours exhibited by these systems towards adduct formation were analyzed in detail².

The formation of pyridine-type base adducts of dithiophosphato, dithiophosphinato and xanthato complexes of nickel(II) has been extensively studied³⁻⁶. The properties of the resulting adducts were often different from those of the parent complexes⁷. For metal β -ketoenolate complexes are a well-studied class exhibiting such behaviours. For example, the planar, diamagnetic bis(dipivaloylmethane) nickel(II) became paramagnetic, trans-octahedral adduct of pyridine⁸. The C—O stretching frequencies of nickel(II) xanthates shifted considerably (*ca.* 50 cm⁻¹) on adduct formation indicating the change of C—O bond order⁹. This was due to the donation of base electrons to the metal making the complex more ionic in character.

It was observed¹⁰ that the formation of *trans*-bis-pyridine adduct of bis(O,O'-diethyl dithiophosphato) nickel(II), [Ni{S₂P(OC₂H₅)₂]₂] distorted the chelate rings without affecting their coplanarity. The Ni—S bond length and the S—P—S bond angle were increased while the S—Ni—S bond angle was decreased. The increase of P—S bond length was, however, negligible. These structural changes which cause the changes in the properties of the resulting adduct were attributed to the decrease of net positive charge on the nickel atom and the increase of net negative charges on the sulfur atoms. The present paper deals with a comparative EHMO and NCA studies of [Ni{S₂P(OC₂H₅)₂]₂] and its pyridine adduct describing the effect of adduct formation on the bonding characteristics of these systems. The results of the EHMO calculations are correlated by relevant force constants calculated from NCA.

EXPERIMENTAL

The adduct [Ni{S₂P(OC₂H₅)₂]₂·2Py] was prepared by the method reported elsewhere¹⁰. The IR spectrum (Fig. 1) of the complex as KBr pellets was recorded in the range 4000–200 cm⁻¹ on a Perkin-Elmer 883 IR spectrometer.

The EHMO calculations were carried out by successively operating CACAO and ICON8 computer programs^{11, 12}. The Wilson GF matrix method¹³ was used to carry out the NCA using "QCMP067 General Vibrational Analysis" program¹⁴. The potential energy matrix (F) was constructed by Urey-Bradley force field¹⁵. The initial assumed set of force constants were refined by the procedure of Nelder and Mead¹⁶. The observed frequencies were assigned by potential energy distribution (PED) calculations (Table-1)¹⁷.

EHMO calculations: The structural parameters (Table-2) of [Ni{S₂P(OC₂H₅)₂]₂] and [Ni{S₂P(OC₂H₅)₂]₂·2Py] (Fig. 2 a and b) were taken from published literature¹⁰⁻¹⁸. The mean values of the bond lengths and bond angles of similar kinds were considered. The H atoms of the pyridine molecules and the C₂H₅ groups of the dithiophosphate fragments were ignored to simplify the calculations. The cartesian coordinates of the atoms required for the calculations were determined by a preliminary run of CACAO and then used as input data in the ICON8 program.

TABLE-1
 POTENTIAL ENERGY DISTRIBUTION (PED) OF $[\text{Ni}\{\text{S}_2\text{P}(\text{OC}_2\text{H}_5)_2\}_2 \cdot 2\text{Py}]$

Species	Symmetry coordinates	Observed frequencies (cm^{-1})			
		810	540	340	328
A ₁	$S_1 = \frac{1}{\sqrt{2}}(dr_1 + dr_2)$	0.000	0.000	0.862	0.006
	$S_2 = \frac{1}{\sqrt{2}}(dr_3 + dr_4)$	0.226	0.750	0.000	0.000
	$S_3 = \frac{1}{\sqrt{2}}(dr_5 + dr_6)$	0.740	0.174	0.000	0.000
	$S_4 = \frac{1}{\sqrt{2}}(dr_7 + dr_8)$	0.000	0.000	0.005	0.992
B ₁		760	630	181 ^a	
	$S_5 = \frac{1}{\sqrt{2}}(dr_5 - dr_6)$	1.000	0.000	0.049	
	$S_6 = \frac{1}{\sqrt{2}}(dr_7 - dr_8)$	0.000	0.961	0.000	
	$S_7 = \frac{1}{2}(d\theta_5 - d\theta_6 + d\theta_7 - d\theta_8)$	0.000	0.000	1.049	
B ₂		670	318	203 ^a	
	$S_8 = \frac{1}{\sqrt{2}}(dr_1 - dr_2)$	0.001	0.835	0.027	
	$S_9 = \frac{1}{\sqrt{2}}(dr_3 - dr_4)$	0.928	0.003	0.018	
	$S_{10} = (d\theta_5 + d\theta_6 - d\theta_7 - d\theta_8)$	0.018	0.085	0.928	

^a Calculated frequencies.

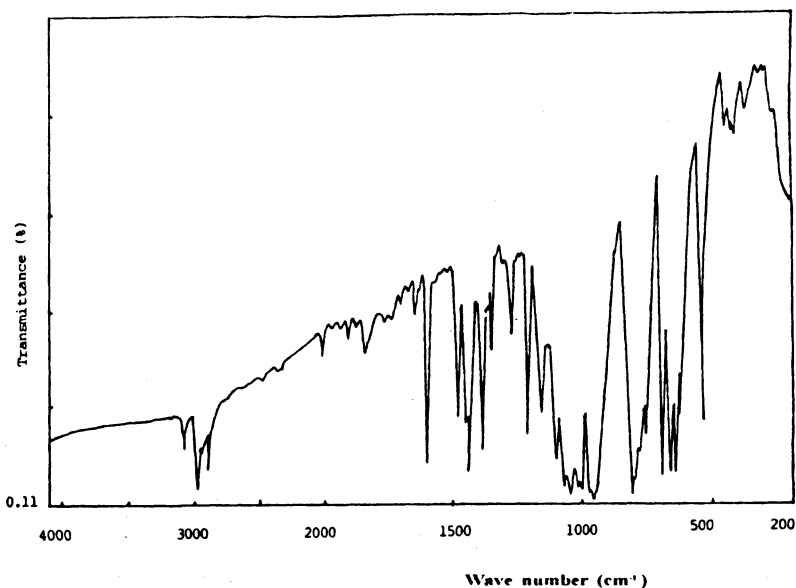


Fig. 1. IR spectrum of $[\text{Ni}\{\text{S}_2\text{P}(\text{OC}_2\text{H}_5)_2\}_2 \cdot 2\text{Py}]$

Table-2
INTERNAL COORDINATES OF
(a) $[\text{Ni}\{\text{S}_2\text{P}(\text{OC}_2\text{H}_5)_2\}_2]$ AND (b) $[\text{Ni}\{\text{S}_2\text{P}(\text{OC}_2\text{H}_5)_2\}_2\cdot 2\text{Py}]$

(a) $[\text{Ni}\{\text{S}_2\text{P}(\text{OC}_2\text{H}_5)_2\}_2]$	(b) $[\text{Ni}\{\text{S}_2\text{P}(\text{OC}_2\text{H}_5)_2\}_2\cdot 2\text{Py}]$
Bond lengths (Å)	Bond lengths (Å) (Mean)
Ni—S = 2.333	Ni—S = 2.495
P—S = 1.989	P—S = 1.985
P—O = 1.575	P—O = 1.585
	Ni—N = 2.110
Bond angles (degree)	Bond angles (degree) (Mean)
$\angle\text{SNiS} = 88.5$	$\angle\text{SNiS} = 81.70$
$\angle\text{NiSP} = 84.5$	$\angle\text{NiSP} = 83.95$
$\angle\text{SPS} = 103.1$	$\angle\text{SPS} = 110.40$
$\angle\text{SPO} = 114.4$	$\angle\text{SPO} = 112.90$
$\angle\text{OPO} = 96.6$	$\angle\text{OPO} = 94.00$
	$\angle\text{SNiS} = 90.35$
	$\angle\text{NCC} = 123.35$
	$\angle\text{CCC} = 118.60$

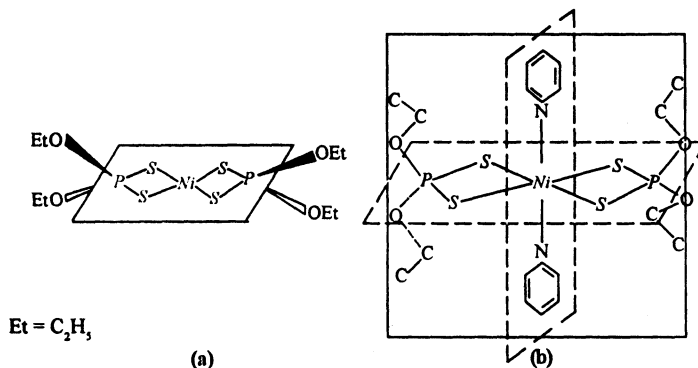


Fig. 2. Structures of $[\text{Ni}\{\text{S}_2\text{P}(\text{OC}_2\text{H}_5)_2\}_2]$ and $[\text{Ni}\{\text{S}_2\text{P}(\text{OC}_2\text{H}_5)_2\}_2\cdot 2\text{Py}]$

Normal Coordinate Analysis: The simplified model (Fig. 3) of the adduct was considered for NCA assuming the $\text{C}_2\text{H}_5\text{N}$ and OC_2H_5 groups to behave as single atoms X and Y with molecular masses of 79 and 45 amu respectively. This eight-atom model contains 21 internal coordinates having the following mean values of the molecular parameters¹⁰:

$r_1 = r_2 = 2.495 \text{ \AA}$, $r_3 = r_4 = 1.985 \text{ \AA}$, $r_5 = r_6 = 1.589 \text{ \AA}$, $r_7 = r_8 = 2.11 \text{ \AA}$,
 $\theta_1 = 81.7^\circ$, $\theta_2 = \theta_4 = 83.95^\circ$, $\theta_3 = 110.4^\circ$, $\theta_5 = \theta_6 = \theta_7 = \theta_8 = 112.9^\circ$, $\theta_9 = 94^\circ$ and
 $\theta_{10} = \theta_{11} = \theta_{12} = \theta_{13} = 90^\circ$.

The 18 normal modes of vibrations ($3N = 6$, $N = 8$) of this model of C_{2v} point group were classified into $8A_1 + 2A_2 + 4B_1 + 4B_2$ symmetry species. However,

the two IR inactive torsional vibrations, $\rho_t(\text{O—P—O})$ and $\rho_t(\text{N—Ni—N})$, of A_2 species were not observed. The calculated and the observed frequencies as well as the refined force constants of the adduct have been compared with the corresponding values¹⁹ of $[\text{Ni}\{\text{S}_2\text{P}(\text{OCH}_3)_2\}_2]$ (Tables 3 and 4) assuming OCH_3 and OC_2H_5 to be equivalent.

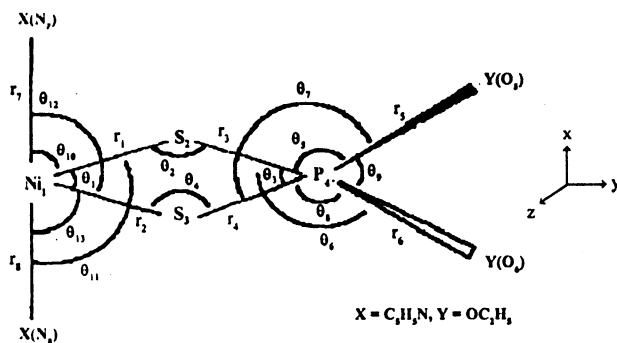


Fig. 3. Molecular model of $[\text{Ni}\{\text{S}_2\text{P}(\text{OC}_2\text{H}_5)_2\}_2 \cdot 2\text{Py}]$

TABLE-3
OBSERVED AND CALCULATED FREQUENCIES OF
(a) $[\text{Ni}\{\text{S}_2\text{P}(\text{OC}_2\text{H}_5)_2\}_2 \cdot 2\text{Py}]$ AND (b) $[\text{Ni}\{\text{S}_2\text{P}(\text{OCH}_3)_2\}_2]$ ¹⁹
WITH BAND ASSIGNMENT AND PED (%)

$[\text{Ni}\{\text{S}_2\text{P}(\text{OC}_2\text{H}_5)_2\}_2 \cdot 2\text{Py}]$				$[\text{Ni}\{\text{S}_2\text{P}(\text{OCH}_3)_2\}_2]$ ¹⁹			
Frequency (cm^{-1})				Frequency (cm^{-1})			
Obs.	Cal.	Assignments	PED (%)	Obs.	Cal.	Assignments	PED (%)
A ₁	810	812 $\nu_s(\text{P—O}) + \nu_s(\text{P—S})$	74, 23	A ₁	823	831 $\nu_s(\text{P—O}) + \nu_s(\text{P—S})$	109, 50
	540	524 $\nu_s(\text{P—S}) + \nu_s(\text{P—O})$	75, 17		519	523 $\nu_s(\text{P—S}) + \nu_s(\text{P—O})$	100, 14
	400	—	—		395	$\delta(\text{O—P—O}) + \delta(\text{S—P—S})$	100, 13
	340	337 $\nu_s(\text{Ni—S})$	86		355	350 $\nu_s(\text{Ni—S})$	100
	328	324 $\nu_s(\text{Ni—N})$	99		252	243 $\delta(\text{S—P—S}) + \delta(\text{O—P—O})$	100, 18
B ₁	760	755 $\nu_a(\text{P—O})$	100	B ₁	796	792 $\nu_a(\text{P—O})$	100
	630	634 $\nu_a(\text{Ni—N})$	96		189	194 $\rho_f(\text{PO}_2)$	100
	—	181 $\rho_f(\text{PO}_2)$	100		189	194 $\rho_f(\text{PO}_2)$	100
B ₂	670	685 $\nu_a(\text{P—S})$	93	B ₂	657	658 $\nu_a(\text{P—S})$	100
	318	314 $\nu_a(\text{Ni—S})$	83		328	327 $\nu_a(\text{Ni—S})$	100
	—	203 $\rho_\omega(\text{PO}_2)$	100		214	214 $\rho_\omega(\text{PO}_2)$	100

TABLE-4
FORCE CONSTANTS 'f' (mdyn/Å)
FOR $[\text{Ni}\{\text{S}_2\text{P}(\text{OC}_2\text{H}_5)_2\}_2\cdot 2\text{Py}]$

The values within the parentheses represent force constants of $[\text{Ni}\{\text{S}_2\text{P}(\text{OCH}_3)_2\}_2]$.

Stretching	
$f_{\text{NiS}} = 1.15$ (1.20)	$f_{\text{PO}} = 6.70$ (3.46)
$f_{\text{PS}} = 4.07$ (2.80)	$f_{\text{NiN}} = 4.90$
Bending	
$f_{\text{SNIS}} = 1.20$ (0.30)	$f_{\text{SPO}} = 0.03$ (0.05)
$f_{\text{NiSP}} = 0.55$ (0.12)	$f_{\text{OPO}} = 0.55$ (0.39)
$f_{\text{SPS}} = 0.09$ (0.15)	$f_{\text{SNIN}} = 0.95$
Repulsive	
$f_{\text{S...S}} = 0.05$ (0.05)	$f_{\text{O...O}} = 0.45$ (0.40)
$f_{\text{Ni...P}} = 0.02$ (0.35)	$f_{\text{S...N}} = 0.01$
$f_{\text{S...O}} = 0.33$ (0.23)	

RESULTS AND DISCUSSION

EHMO calculation: The paramagnetic character¹⁰ of the adduct is revealed by the one-electron occupation of its highest occupied molecular orbital (Ψ_{HOMO}). The fragment molecular orbital (FMO) analysis has shown that the HOMO of the adduct is formed by the bonding interaction between $\text{Ni}(d_z^2)$ and $\text{N}(p_z)$ associated with a flow of electrons from the HOMO (ϕ_{HOMO}) of the pyridine fragment to the lowest unoccupied molecular orbital (ϕ'_{LUMO}) of the $[\text{Ni}\{\text{S}_2\text{P}(\text{OCH}_3)_2\}_2]$ (Fig. 4) which is consistent with the fact^{20, 21} that nickel dithiophosphates were used as reference acceptors in the determination of many thermodynamic constants. The other bonding molecular orbitals are formed by the interactions of p_x and p_y orbitals of pyridine nitrogen with d_{xz} and d_{yz} orbitals, respectively, of the nickel atom. However, these interactions, which are of π -character, are expected to be very small as the Ni—N bonds in the adduct do not have any double bond character¹⁰. The adduct formation is associated with a decrease in the net positive charge on the nickel atom and a simultaneous increase of net negative charges on the sulfur atoms (Table-5). The former effect increases the Ni—S bond length¹⁰ resulting in a decrease of the reduced overlap population (ROP) between nickel and sulfur atoms (Table 5). The latter effect increases the S—P—S bond angle and also the S—P flow of electrons, which results in a slight decrease of the net positive charge on the phosphorus atom (Table-5). The difference between the P—S bond lengths in $[\text{Ni}\{\text{S}_2\text{P}(\text{OCH}_3)_2\}_2]$ and its pyridine adduct is negligible (Table-2) and the increase of $\text{ROP}_{\text{P-S}}$ (Table-5) in the adduct may be due to the increase of P—S bond order²². The donor solvent molecules (L), that complete the coordination sphere of Ni^{2+} ion in nickel diethyldithiophosphate adduct, $[\text{Ni}\{\text{S}_2\text{P}(\text{OCH}_3)_2\}_2\cdot 2\text{L}]$, also affect the structure of the chelate rings in the same way as mentioned above. As a result of the two opposing effects, that is the

decrease of the S—Ni—S bond angle and a simultaneous increase of S—P—S angle, the Ni—S bonds, which are weaker than the P—S bonds¹⁹, are disrupted in water or other solvents of high dielectric constants²³.

Table-5
NET CHARGES (Q) AND REDUCED OVERLAP POPULATIONS (ROP) OF
[Ni{S₂P(OC₂H₅)₂}₂] AND [Ni{S₂P(OC₂H₅)₂}₂·2Py]

Complex	Net charge (Q)				Reduced overlap population (ROP)			
	Q _{Ni}	Q _S	Q _P	Q _O	Ni—S	P—S	P—O	Ni—N
[Ni{S ₂ P(OC ₂ H ₅) ₂ } ₂]	1.872	-0.013	1.971	-1.440	0.265	0.815	0.590	-
[Ni{S ₂ P(OC ₂ H ₅) ₂ } ₂ ·2Py]	0.877	0.488	1.897	0.723	0.060	0.842	0.562	0.136

Normal Coordinate Analysis: The discussion is based on the assumption that OCH₃ and OC₂H₅ groups are equivalent and have the same effect on the bonding characteristics in the chelate rings of the complexes considered for the present calculation. The agreement between the observed and calculated frequencies (Table-3) of the adduct is quite satisfactory, the maximum deviations being 2.7%. The band assignments are consistent with those¹⁹ of [Ni{S₂P(OCH₃)₂}₂]. The symmetric (ν_{sym}) and antisymmetric (ν_{asym}) P—S stretching vibrations (519 cm⁻¹ and 657 cm⁻¹ respectively) of [Ni{S₂P(OCH₃)₂}₂] have been shifted to 540 cm⁻¹ and 670 cm⁻¹ in the pyridine adduct, [Ni{S₂P(OC₂H₅)₂}₂·2Py] indicating an increase of P—S bond order²². This may be attributed²⁴ to the increase of ionic character of the (Ni—S) bond with increased electron density on the sulfur atoms and a decrease of S → Ni sigma electron flow leading to an overall increase of P—S bond order. This is reflected in the reasonably higher P—S stretching force constant ($f_{\text{P-S}} = 4.07$ mdyne/Å) of the adduct compared to that ($f_{\text{P-S}} = 2.80$ mdyne/Å) of [Ni{S₂P(OCH₃)₂}₂] (Table-4). It may be suggested from the Ni—S bond distances (Table-1) of the present two systems that the (Ni—S) bond in the adduct is somewhat weaker than that of [Ni{S₂P(OCH₃)₂}₂] and this is corroborated by the relative values of their Ni—S stretching force constants (Table-4) as well as the respective values of $\nu(\text{Ni—S})$ (Table-3).

The bands observed at 328 cm⁻¹ and 630 cm⁻¹ in the IR spectrum of the adduct have been assigned to $\nu_{\text{sym}}(\text{Ni—N})$ and $\nu_{\text{asym}}(\text{Ni—N})$ respectively. For the frequencies above 650 cm⁻¹, the pyridine vibrations show very little shift upon complex formation²⁵ and the IR bands observed at 700 cm⁻¹ and 650 cm⁻¹ for the adduct may thus be expected as due to the pyridine vibrations^{26, 27}. The bands at 604 cm⁻¹ (in-plane ring deformation) and 405 cm⁻¹ (out-of-plane ring deformation) of pyridine, however, are shifted to higher frequencies upon coordination to a metal²⁸. The band at 450 cm⁻¹ in the adduct may thus be assigned to the out-of-plane ring deformation vibration of the pyridine molecule, while the band at 630 cm⁻¹ may be due to the antisymmetric (Ni—N) stretching vibration (Table-3) coupled with the in-plane ring deformation vibration of pyridine. The band observed at 400 cm⁻¹ for the adduct corresponds to the band observed at

395 cm^{-1} in case of $[\text{Ni}\{\text{S}_2\text{P}(\text{OCH}_3)_2\}_2]$ assigned to O—P—O bending vibration. The symmetric Ni—N vibration occurs at 328 cm^{-1} which is reasonably higher than the corresponding values²⁹ of $[\text{Ni}(\text{Py})_2\text{I}_2]$ (240 cm^{-1}) and *trans*- $[\text{Ni}(\text{Py})_4\text{Cl}_2]$ (236 cm^{-1}). This large variation in $\nu_{\text{sym}}(\text{Ni—N})$ values may be due to the fact that the metal-pyridine stretching vibrations are very sensitive to the stereochemistry of the complexes²⁹.

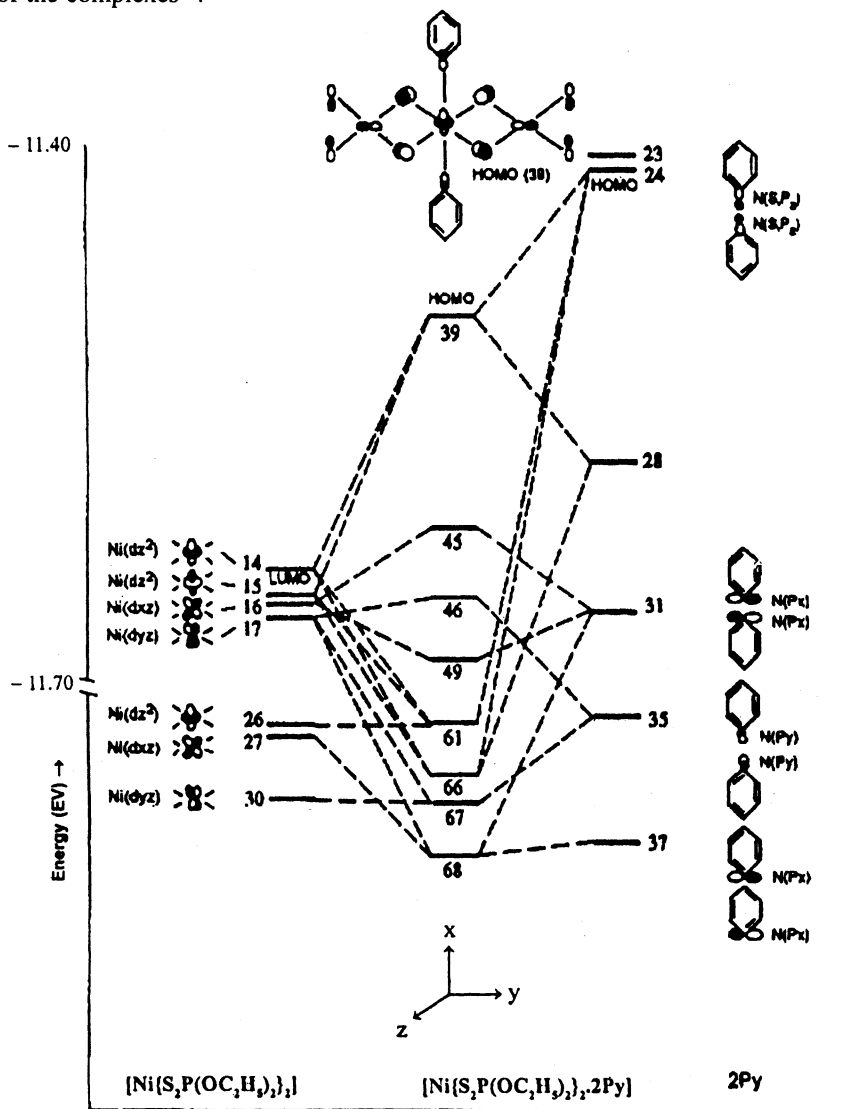


Fig. 4. Interaction diagram of $[\text{Ni}\{\text{S}_2\text{P}(\text{OC}_2\text{H}_5)_2\}_2 \cdot 2\text{Py}]$

Conclusion

The effect of adduct formation by pyridine with $[\text{Ni}\{\text{S}_2\text{P}(\text{OC}_2\text{H}_5)_2\}_2]$ on the bonding characteristics of the parent complex has been discussed on the basis of

HOMO-LUMO interaction, net charges on atoms and reduced overlap populations derived from EHMO calculations. The NCA of the above systems corroborate the observations obtained from EHMO analysis.

ACKNOWLEDGEMENT

We thank University Grants Commission, New Delhi, for financial support in the form of awarding a Visiting Associateship (PKG) and a Teacher Fellowship (RK).

REFERENCES

1. R.L. Carlin and D.B. Losee, *Inorg. Chem.*, **9**, 2087 (1970).
2. P.K. Gogoi and R. Konwar, *Asian J. Phy.* (in press).
3. D.R. Daktenieks and D.P. Graddon, *Aust. J. Chem.*, **24**, 2509 (1971).
4. V.T.P. Anh, D. P. Graddon and V.A.K. Ng, *Aust. J. Chem.*, **31**, 2417 (1978).
5. R.L. Carlin, J.S. Dubnoff and W.T. Huntress, *Proc. Chem. Soc.*, 228 (1964).
6. D.P. Graddon and S. Prakash, *Aust. J. Chem.*, **27**, 2099 (1974).
7. D. Coucouvanis and J.P. Fackler (Jr.), *Inorg. Chem.*, **6**, 2047 (1967).
8. J.T. Hashagen and P. Fackler (Jr.), *J. Am. Chem. Soc.*, **87**, 2821 (1965).
9. A.B. Blake, F.A. Cotton and J.S. Wood, *J. Am. Chem. Soc.*, **86**, 3024 (1964).
10. S. Ooi and Q. Fernando, *Inorg. Chem.*, **6**, 1558 (1967).
11. D.M. Proserpio and C. Mealli, CACAO, P.C. Version 3.0, Instituto di Strutturistica Chimica, Italy (1992).
12. J. Howell, A. Rossi, D. Wallace, K. Haraki and R. Hoffmann, ICON 8, Department of Chemistry, Cornell University, New York.
13. E.B. Wilson (Jr.), J.C. Decius and P.C. Cross, *Molecular Vibrations*, McGraw-Hill Book Co. Inc., New York (1955).
14. D.F. McIntosh and M.R. Peterson, QCMPO67, Department of Chemistry, University of Toronto, Canada (1988).
15. T. Shimanouchi, *J. Chem. Phys.*, **17**, 245 (1949).
16. J.A. Nelder and R. Mead, *Computer Journal*, **7**, 308 (1965).
17. D.N. Sathyanarayana, *Vibrational Spectroscopy, Theory and Applications*, New Age International, New Delhi (1996).
18. J.F. McConnell and V. Kastalsky, *Acta Cryst.*, **B22**, 853 (1967).
19. W. Rudzinski, G.T. Behnke and Q. Fernando, *Inorg. Chem.*, **16**, 1206 (1977).
20. L. Sacconi, G. Lombardo and R. Ciafalo, *J. Am. Chem. Soc.*, **82**, 4182 (1960).
21. L. Sacconi, G. Lombardo and P. Paoletti, *J. Am. Chem. Soc.*, **82**, 4185 (1960).
22. R.N. Mukherjee, P.K. Gogoi and R. Raghunand, *Indian J. Chem.*, **20A**, 688 (1981).
23. P.S. Shetty and Q. Fernando, *J. Inorg. Nucl. Chem.*, **28**, 2873 (1966).
24. S.E. Livingstone and A.E. Mikhelson, *Inorg. Chem.*, **9**, 2545 (1970).
25. N.S. Gill, R.H. Nuttall, D.E. Scaife and D.W.A. Sharp, *J. Inorg. Nucl. Chem.*, **18**, 79 (1961).
26. Wilmshurst and Bernstein, *Can. J. Chem.*, **18**, 1183 (1957).
27. Corrsin, Fax and Lord, *J. Chem. Phys.*, **22**, 2013 (1953).
28. K. Nakamoto, *Infrared Spectra of Inorganic and Coordination Compounds*, 2nd Edn., John Wiley & Sons, New York (1970).
29. R.J.H. Clark and C.S. Williams, *Inorg. Chem.*, **4**, 350 (1965).